Journal of Materials Chemistry B

Accepted Manuscript

ROYAL SOCIETY OF CHEMISTRY

www.rsc.org/materialsB

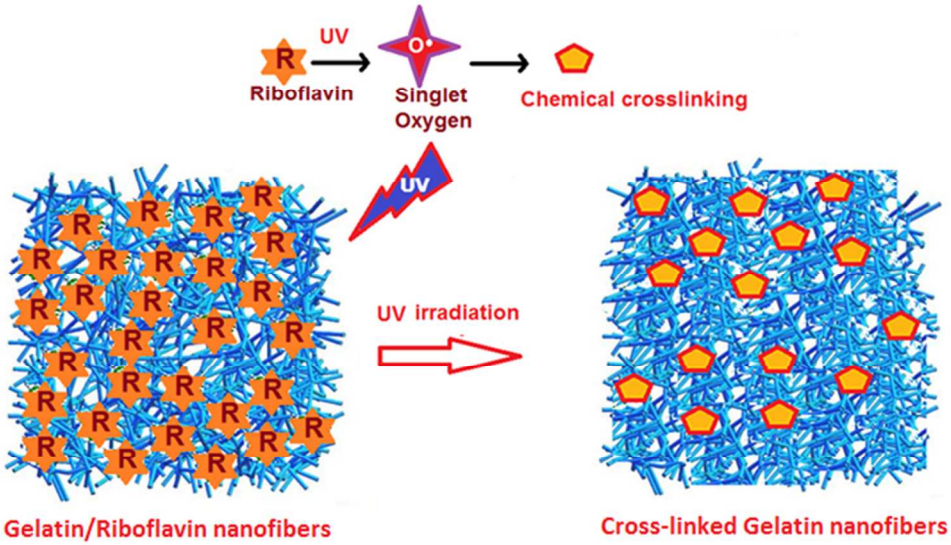

313x172mm (72 x 72 DPI)

Cross-linking of Protein Scaffolds for Therapeutic Applications: PCL Nanofibers Delivering Riboflavin for Protein Cross-Linking

Radhakrishnan Sridhar,[a, b 1]* Kalaipriya Madhaiyan,[c 1] Subramanian Sundarrajan,[a, b] Aleksander Góra [a, b] Jayarama Reddy Venugopal[a, d] and Seeram Ramakrishna[a, b, d]*

[a] *Center for Nanofibers and Nanotechnology, NUSNNI, National University of Singapore.*

[b] *Department of Mechanical Engineering, National University of Singapore.*

[c] *Department of Pharmacy, National University of Singapore.*

[d] *NUS Nanoscience & Nanotechnology Initiative, 117581, Singapore.*

Keywords: Vitamin B_2, Protein, Crosslinking, nanofiber, controlled release.

Corresponding Author: Prof. Seeram Ramakrishna & Dr. Radhakrishnan Sridhar; Fax: +65-6773 0339; E-mail : seeram@nus.edu.sg and rad_sri@yahoo.com

ABSTRACT

Nanofibers play a significant role in tissue engineering and drug delivery because of the ease to incorporate drugs or pharmaceuticals into the nano formulation. Natural protein nanofibers are cross-linked (CXLed) employing a new protocol to improve their stability for perspective usage as tissue engineering or drug delivery scaffolds. The protocol utilizes non-toxic, natural material vitamin based CXL protocol that works well for stabilizing protein nanofibers. We have experimented the generation of reactive oxygen species (ROS) from UV treated Rib-Gelatin microfiber or film or solution that helps in Gelatin (Gel) CXLing and results in improved mechanical properties. Further natural proteins Gel and Fibrinogen (Fib) solutions were also CXLed using the vitamin B_2 (Riboflavin (Rib)) released from Rib loaded Polycaprolactone (PCL) nanofiber followed by UV treatment. The sustained release of Rib from PCL nanofiber is studied with *in vitro* drug release experiments and *in vitro* hydrogel formation upon treatment with the natural protein solutions. Rib loaded nanofibers were characterized with SEM and AFM for morphology, mechanical strength calculation and FT-IR for ensuring drug incorporation. The Rib encapsulation in the nanofiber reservoirs enables the sustained release and the ROS generating nanofiber could find application as a patch for CXLing any protein fiber or fibrous tissue, such as ocular, skin, cardiac tissue engineering.

INTRODUCTION

Nanotechnology based drugs and medical devices are increasing in number as a remedy for growing unmet medical needs [1-3]. Sustained release of drugs from nanotechnology based polymeric drug delivery systems with relevant physico-chemical properties improve programmed release of drugs, bioavailability and therapeutic efficacy of drugs [4-6]. Electrospun nanofibers found applications in many areas and their application in biomedical and pharmaceutical applications is overwhelming [7-13]. Nanofibrous scaffolds constitute potential solutions in wound healing, tissue regeneration and drug delivery applications [14-16]. The biomimetic electrospun nanofiber membranes (NFM) express the regenerated extracellular matrix (ECM) that support in cell proliferation and stem cell differentiation in tissue engineering [17, 18]. Further the natural polymer nanofibers find use in drug delivery systems and are beneficial for sustained release of drug [19, 20] component which finally degrade totally. The main issue with application of natural materials in tissue engineering or drug delivery applications is their poor stability and mechanical properties as they are fast biodegradable. CXLing of these proteins was carried out in order to enhance the mechanical stability of the protein nanofibrous scaffolds [21] and to reduce the rate of biodegradation. The CXLing interconnects protein nanofibers together, improves the mechanical strength of the scaffold and improves aqueous stability. Protein CXLing was commonly carried with glutaraldehyde [22], genipin [23] or with N-(3-Dimethylaminopropyl)-N'-ethylcarbonate (EDC) [24]. Among these glutaraldehyde route holds more promise because of its in-expensive, efficient, and wide range amine group specific reactivity. But the cytotoxity [25] and calcification [26] issues associated with this fixation agent limit its versatile applicability.

Riboflavin (Rib) or Vitamin B_2, is a water-soluble nutrient [27], plays a significant role in metabolization of carbohydrates, protein, or fat by the cells and to create energy. Rib exhibits

critical role for normal reproduction, cell growth and repair, and development of tissues. Further body utilizes the vitamin to keep tissue healthier and for wound healing [28].

We herein put forward the new concept of CXLing natural protein nanofibers using Rib following UV treatment and demonstrated the concept with Gel CXLing in nanofibers, film and solution. The hypothesis behind the concept is the liberation of ROS upon treatment of Rib loaded protein nanofibers with UV which then CXLs or interconnects the proteins (Figure 1). Long wave ultra violet irradiation (UVA) mediated generation of ROS from Rib solution and assisted collagen CXLing phenomenon [29-35] is a well-established in corneal collagen CXLing and a proven method of treatment for keratoconus, bulging of corneal collagen fibers. A typical corneal collagen CXL treatment requires 0.1 % of Rib concentration during UV CXLing time of 30 minutes and as a result collagen CXL happens, cornea becomes thinner curing keratoconus. Herein we attempt to fabricate Rib mediated, CXLed Gel scaffolds and our present demonstration of ROS mediated CXL will outdate the usage of cyto-toxic glutaraldehyde for CXLing protein nanofibers, films and solutions. Rib loaded nanostructured systems were reported for corneal absorption and trans-epithelial collagen CXL [36, 37]. And there is still a need for Rib delivery systems that could CXL natural fibrous protein tissue scaffolds that constitute dentins, ocular components, and pericardium. To be applicable as a new mode of administration for similar CXLing applications we formulated nanofibrous Rib delivery system and demonstrated *in vitro* protein CXLing. The *in vitro* sustained release of the CXLer from Rib-PCL nanofiber was studied and its ability to CXL natural proteins *in vitro* in solutions was analyzed.

EXPERIMENTAL

Materials

PCL (Mw = 80,000), Gelatin, Riboflavin (B_2 Vitamin), Glutaraldehyde, Chloroform and Methanol were purchased from Sigma-Aldrich (Singapore). All chemicals were of analytical grade and used without further purifications.

Preparation of nanofibrous and as cast membranes

Preparation of electrospinning solutions: PCL (1 g) was dissolved in 10 mL of Chloroform/Methanol (3 : 1 v/v) to prepare the spinnable polymer solution at a concentration of 10% w/v at ambient temperature. After 3 hours stirring time to obtain a transparent PCL solution, Rib (50 mg) was loaded in to PCL solution by suspending solid Rib at the amount of 5 wt% with respect to PCL. The mixture was stirred overnight at room temperature to obtain a homogenous yellow colored solution. PCL solution (10%) void of the vitamin was used to prepare the control PCL nanofibers. For preparing the Rib-Gel microfibers, Gel (1 g) was dissolved in 10 g of Trifluoroethanol at a concentration of 10% w/v. After stirring at ambient temperature for 3 hours, Rib was loaded in to Gel solution by dissolving its powder in varying amount of 0.1, 1 and 5 wt% with respect to Gel. The mixture was stirred overnight at room temperature to achieve a homogenous solution. Pure 10% Gel solution was used for preparing the Gel microfibers which served as control. For serving as a positive control for Glutaraldehyde vapor CXLing was used and was done according to the procedure reported in the literature [38].

Electrospinning processing

A high voltage DC power supply (from Gamma High Voltage Research, Florida, U.S.) was used to provide high voltages in the range of 10–30 kV. The polymer PCL solution was poured into a standard 10 ml syringe that was attached to a steel needle. Electrospinning was

carried out by introducing the high voltage to the needle as a positive electrode and a fixed sheet of grounded aluminum collector. The distance between needle tip and collector was adjusted to 15 cm so as to obtain bead less nanofibers. Once positive electrode reached a critical voltage of 15 kV, spinning head extruded polymer solution and the bead less electrospun PCL or Rib-PCL nanofibers were deposited on the aluminum foil collector. The emitting rate of the polymer solution was controlled to 1.5 ml/h by means of a syringe pump (KD Scientific Inc., M.A., U.S.). The same protocol is used to prepare the Gel or Rib-Gel microfibers (in varying concentrations of vitamin) with distance of electrospinning at 12 cm, applied voltage 10 kV and Gel solution flow rate of 0.5 mL per hour. The as cast Gel or Rib-Gel films were fabricated using the same solutions used for electrospinning the nanofibers. For hydrogel formation studies of 5 % Gel aqueous solution was prepared with varying concentrations of Rib. For Rib-PCL nanofiber mediated CXLing and Gel or Fib hydrogel formation, 5 % aqueous Gel or Fib solutions were treated with 1% Rib-PCL nanofiber.

UV light mediated CXLing of Gel microfibers, films and protein solutions

Fabricated electrospun or as cast films are vacuum-dried at room temperature and characterized without further chemical treatment for stabilizations of the membranes. UV CXLing of Gel microfibers and as cast films was achieved invariably with 30 minutes UV treatment of these samples in sterilization laminar flow hood. The aqueous Gel (5%) solutions were CXLed to result hydrogels with varying time interval of UV treatment. The Fib or Gel solutions are inserted with the Rib-PCL nanofiber and UV treated for 3 hours' time. Then the Fib or Gel hydrogel was freeze-dried and characterized.

Surface modification

PCL nanofibers was surface plasma treated with an electrode-less, inductively coupled radio-frequency glow discharge (RFGD) plasma cleaner (PDC-001; Harrick Plasma, Ithaca, NY),

at varying time intervals. The air plasma treatment was carried out for 5, 10, 20, 30, 40 and 60 seconds time intervals with the radio-frequency power set at 30 W. The surface hydrophilicity and resulting drug release kinetics of the plasma treated and plasma untreated samples were compared.

Characterization; Surface morphology, Chemical and mechanical

Hydrophilicity of the electrospun B_2 loaded PCL fibrous membranes was measured and compared with the use of a video contact angle instrument (VCA-optima, AST, Inc.). Deionized water (25 μL) was automatically dropped onto the flat fibrous membranes. The contact angles indicating the wetting ability of the materials were calculated automatically. The surface morphology of the electrospun nanofibers was studied with a JEOL JSM-5900 scanning electron microscope (Quanta 200F, FEI, Oregon, US) and atomic force microscopy (AFM). Gold sputtered (JEOL JFC-1200 fine coater, Japan) NFMs were observed under SEM to study the nanofiber morphology and nanofiber diameter. Image-J (National Institutes of Health, USA) image visualization software was applied to measure the nanofiber diameter. The average of 30 nanofibers chosen from the SEM micrographs at random was measured as nanofiber diameter. AFM images were processed with JPK data processing software was used to process the AFM images and to measure the surface roughness of the nanofiber or thin films. Fourier-transform infrared (FTIR) spectra were obtained on a Avatar 380 spectrometer, (Thermo Nicolet, Waltham, MA, USA) in Attenuated total reflectance (ATR) mode. The scanning range was 750–4000 cm^{-1} and the resolution was 1 cm^{-1}. Mechanical properties of electrospun fibrous membranes were determined with a tabletop uniaxial tensile testing machine (INSTRON 3345, USA) with the use of a 10 N load cell under a cross-head speed of 5 mm/min at ambient conditions. All samples were prepared in the form of rectangular shape with dimensions of 20-10 mm from the electrospun fibrous membranes.

The thicknesses of samples were measured with a digital micrometer. At least five samples were tested for each type of electrospun fibrous membranes.

***In vitro* Rib drug release studies**

The release profile of B_2 from the Rib- PCL nanofibers was investigated in PBS at pH 7.4. Each drug-loaded fiber sample (~20mg) was incubated at 37 ^{o}C in 20 mL of the aforementioned release medium under stirring. Aliquots of samples (1 mL) were taken from the release medium at specific time intervals and that volume was replaced with fresh PBS. The amount of B_2 released at various times, up to 48 h, was determined using an ultraviolet-visible (UV–Vis) spectrometer at excitation of 365 nm. Each drug release experiment was carried out in independent triplicate. With the aid of the calibration curve of B_2 measured in the same condition, the percentage of B_2 release was calculated and plotted versus time according to the equation

Vitamin Release (%) = (Released B_2/ Total loaded B_2) X 100 (%).

RESULTS AND DISCUSSION

Surface morphology of PCL nanofibers and Gel microfibers

The surface morphology of Rib loaded nanofibers was studied with SEM (Figure 2a-f). Both the SEM images of the 1% Rib loaded Gel were micron size fibers (Figure 2a & 2b). When the UV untreated fiber showed 2.18±0.3 μm fiber diameter, the UV treated Rib-Gel microfibers showed 1.749±0.25 μm fiber diameter. The SEM images of the 1% Rib loaded Gel microfibers with and without UV treatment showed slight reduction in fiber diameter in the case of UV treated Rib-Gel microfiber. It can be realized that the UV mediated ROS generation or assisted CXLing reduces protein scaffold fiber diameter significantly. And there was a reduction of roughness in the case of UV treated 5% Rib-Gel as-cast film in comparison with the UV untreated film (Figure 2c & 2d). Bead less 1% Rib-PCL nanofibers

(Figure 2e & 2f) were obtained with fiber diameter distribution in 270 nm range. (ie., mean fiber diameter = 267 ± 37 nm). AFM image (Figure 2g & 2h) of 5 % Rib-Gel NFMs showed fiber diameter in the range 2.6 μm and it was observed that the fiber diameter increases with the percentage increase in the Rib addition. From the AFM images the nanofiber surface root mean square (RMS) roughness (Rq) was found to be 820 nm and average roughness (Ra) was found to be 649 nm. In UV light the Rib-PCL NFM was green emitting and photoluminescence spectra by excitation at 350 nm showed emission maxima at 700 nm. Riboflavin released from 1% Rib-PCL nanofibers is evidenced by CXLing and hydrogel formation of protein solutions Fibrinogen (Fib) and Gelatin (Gel). The SEM images (Figure 3a & 3b) of the freeze-dried CXLed hydrogels show microporous structure formation similar to honey comb in the case of CXLed Fib and porous mesh in the case of CXLed Gel.

FT-IR spectrum showing crosslinking of protein nanofibers

The Rib release from the PCL nanofiber and mediated CXLing was further evidenced from the FT-IR spectra (Figure 3c & 3d) of the freeze-dried protein hydrogel. The IR spectra of non CXLed Fib show Fib amide I, amide II and amide III appear at 1635, 1542 and at 1403 cm^{-1} respectively. The corresponding peaks appear with a slight shift for the Rib CXLed protein except for the amide III peak at 1403 cm^{-1}. The peak around 1250 cm^{-1} was due to presence of Rib released from Rib-PCL nanofibrous membrane in the fibrinogen hydrogel and due to its crosslinking with the protein.

The IR spectra (Figure 4) of the vitamin loaded sample revealed the presence of characteristic Rib amide, imide bonds C=O stretching [39] around 1750 cm^{-1} to 1650 cm^{-1} and the pyrazine ring bond was found at 1520 cm^{-1}. The aliphatic CH bonds were realized at 3000 cm^{-1} and the amine of Gel or OH bonds of Rib around 3400 cm^{-1}. Gelatin amide I, II, and III bands occur at 1643, 1541 and at 1240 cm^{-1} in the Rib-Gel microfibers. After UV CXLing there was a

formation of new peak around 1610 and at 1256 cm^{-1} which might be resulting from the CXLed imidazolone products and aldol crosslinking products [40].

Hydrophilicity of Rib-PCL nanofibers and the release profile of vitamin

The hydrophilicity of the Rib-PCL-NFM was noted with contact angle measurements (Figure 5a) as a comparison between the control PCL, 5% Rib-PCL and plasma treated 5% Rib-PCL samples. Except the control and plasma untreated Rib-PCL samples all the other five plasma treated samples are wettable within a maximum of 25 min time. The 5 seconds plasma treated sample took the maximum time to get wetted whereas the 40 seconds plasma treated sample was wetted within 3 min time. The plasma untreated sample exhibited slow and gradual increase in hydrophilicity which extended beyond 100 min time to get fully wetted and the control PCL remained hydrophobic with a slight reduction in hydrophobicity. Even with 5% of the vitamin loaded nanofibers, the hydrophilicity of Rib-PCL NFM got reduced in terms of contact angle from 140 degrees to 60 degrees in 100 minutes time which is lesser than 50% reduction of the initial contact angle. After 30 minutes of initial fast increase in hydrophilicity further reduction was slow and is due to the hydrophobicity of PCL polymer. This could enable slow release of the drug from the nanofibers. Cumulative drug release studies (Figure 5b) from the Rib-PCL nanofibers were carried out with immersing 20 mg of the vitamin loaded nanofibers in to 1X PBS solution in vitro. The drug release profiles of plasma treated Rib-PCL nanofibers are compared with plasma untreated Rib-PCL nanofibers. The drug released from the plasma untreated sample showed initial slow release of vitamin and showed increased release during 12 to 24 hours' time. After one day incubation the membrane showed only marginal release of vitamin and reached 30% after 2 days. The 20 seconds plasma treated sample exhibited initial burst release in 4 hours' time with 25% of drug released but release rate got reduced during the next 8 hours and reached near maximum after 12 hours. Both 40 seconds and 60 seconds plasma treated samples showed similar release

profile as that of 20 seconds plasma treated sample but with an increased release profile. Almost 92% drug release was noted for 60 seconds plasma treated sample and 82% for the 40 seconds plasma treated samples. The percentage drug released from the plasma treated samples show more drug release when compared to untreated sample. Further increase in plasma treatment duration increased the percentage of drug released from the NFM. The observed results proved that with decrease in water contact angle or in other words with increase in hydrophilicity the percentage drug released increases. The drug released from the nanofibers was mediated by water sorption in to the nanofiber nano-pores which results in water soluble vitamin desorption from the hydrophobic polymer nanofibers. The vitamin was released exponentially from the nanofiber reservoir and reached a steady state after 24 hours for the plasma untreated samples. For the plasma treated samples the steady state release was attained in much earlier time, after 12 hours. The morphologies of the 2 months degraded samples in PBS buffer medium were compared as an effect of hydrophilicity. The SEM images of 5% Rib-PCL NFMs, it can be inferred that the plasma treated sample showed (Figure 6) more degradation with more surface erosion as an effect of more diffused or desorbed drug and the plasma untreated sample showed relatively less degradation.

Mechanical strength to evidence crosslinking of protein scaffolds

Mechanical strengths of Rib-Gel microfibers with varying concentrations of vitamin and with varying duration of UV treatment were compared as a measure of ROS mediated CXLing ability of Rib. The 60 min Glutaraldehyde vapor CXLed Gel microfiber was compared as a positive control with the Rib CXLed Gel microfiber samples. Uniaxial tensile strength measurements of Rib-Gel microfibers (Figure 7a) showed with increase in UV CXLing time the Young's modulus increased within the same concentration set (Figure 7b). There was approximately a five times increase in Young's modulus of the Rib-Gel NFMs with 1 hr UV treatment. Upon increasing concentration of vitamin, CXLing or Young's modulus improved

among the similar UV CXLed samples. The increase was three times in Young's modulus without UV treatment just with increase in the amount of vitamin. This increase in tensile strength with increase in concentration of Rib loading and without any UV treatment can be attributed to the residual ROS released during sample preparation and associated CXLing. In comparison with the positive glutaraldehyde control both the 60 min CXLed 0.1% and 1 % Rib-Gel microfiber samples showed higher Young's modulus. Also the 30 min CXLed 5% Rib-Gel sample was showing higher Young's modulus than the positive control. This clearly indicates that the even lesser percentage of Rib can be used for CXLing protein nanofiber samples with no need for the cytotoxic CXLer glutaraldehyde. We have used AFM surface roughness as a tool to study the mechanical strength resulted from ROS CXLing. The AFM morphology and roughness of the membrane surface was compared between the 5% Rib-Gel microfibers (Figure 8a & 8b) and films. In both cases the roughness decreases as a measure of increase in mechanical strength (Figure 8c) up on UV treatment of the Rib-PCL nanofibers or films due to CXLing. This is due to the dense packing of protein fibers or films upon CXLing in comparison with the samples without CXLing. Further to show the CXLing effect of Rib, Gel solution was treated with varying quantities of Rib and with varying CXLing time intervals (Figure 9). Gel solution with 1% Rib became complete gel after 30 min UV CXLing. 0.5% and 0.3% Rib solutions became complete hydrogel after 1 hr and 2 hrs respectively, while 0.2 % took 3 hrs time UV CXLing. Complete gelation occurred from 0.1 % concentration of Rib after 24 h UV CXLing. CXLing of Gel is mediated by singlet oxygen generation from the Rib upon UV treatment similar to collagen CXLing in keratoconus treatment. Thus the protocol was helpful to CXL protein nanofibers successfully without any incorporation of synthetic polymers for perspective fabrication of tissue engineering or drug delivery scaffolds.

CONCLUSION

The sustained release of water soluble vitamin B_2 is demonstrated from the hydrophobic PCL polymer nanofiber matrices. It was shown with mechanical strength measurement that upon UV treatment, the Rib generates singlet oxygen radicals that assist CXLing of Gel microfibers. Further the same phenomenon is supported by the formation of hydrogel from Gel solution using various amounts of vitamin B_2 and by varying time intervals of UV irradiation. The AFM experiments also confirmed the CXLing hypothesis by the reduction of surface roughness in the Rib-Gel NFM and in as-cast films. We herein for the first time attempted the stabilization of nanofibrous protein scaffolds with Rib and UV mediated CXLing. With the obtained results we conclude that the protein or amine nanofibers can be CXLed with the application of this novel CXLing protocol. This method of CXLing mediated by natural vitamin is most importantly less-toxic and commercially economic. This could potentially replace other CXLing protocols available for protein nanofiber stabilization and thus could serve as a vital tool for drug delivery and tissue engineering researchers. Apart from protein scaffolds CXLing our future interests will be the Rib-PCL nanofiber mediated CXLing of natural protein tissues intending biomedical applications.

ACKNOWLEDGEMENT

This study was supported by the Ministry of Education (R-265-000-318-112), NRF-Technion (R-398-001-065-592), A*STAR-BEP (R-265-000-437-305) and NUS, Singapore.

REFERENCES:

1. T. Kubik, K. Bogunia-Kubik and M. Sugisaka. *Curr Pharm Biotechnol*., 2005, **6**, 17-33.
2. K. K. Jain. *Drug Discov. Today*, 2005, **10**, 1435-1442.
3. M. Chakraborty, S. Jain and V. Rani. *Appl Biochem Biotechnol*., 2011, **165,** 1178-1187.
4. S. E. Leucuta. *Curr Clin Pharmacol*., 2010, **5**, 257-280.
5. A. J. McHugh. *J Contrl Rel*., 2005, **109**, 211-221.
6. P. Agarwal and I. D. Rupenthal. *Drug Discov. Today*, 2013, **18**, 337-349.
7. A. Greiner and J. H. Wendorff. *Adv Poly Sci*., 2008, **219**, 107-171.
8. G. Wei and P. X. Ma. *Adv Functl Mat*., 2008, **18**, 3568-3582.
9. A. Martins, R. L. Reis and N. M. Neves. *Intl Mat Rev*., 2008, **53**, 257-274.
10. M. Hadjiargyrou and J. B. Chiu. *Exp Opin Drug Deliv*., 2008, **5**, 1093-1106.
11. G. R. Williams, N. P. Chatterton, T. Nazir, D. G. Yu, L. M. Zhu and C. J. Branford-White. *Therap Deliv*., 2012, **3**, 515-533.
12. R. Jayakumar, D. Menon, K. Manzoor, S. V. Nair and H. Tamura. *Carbo Poly*., 2010, **82**, 227-232.
13. S. Chakraborty, I. C. Liao, A. Adler and K. W. Leong. *Adv Drug Deliv Rev*., 2009, **61**, 1043-1054.
14. R. Sahay, P. Suresh Kumar, R. Sridhar, J. Sundaramurthy, J. Venugopal, S. G. Mhaisalkar and S. Ramakrishna. *J. Mater. Chem*., 2012, **22**, 12953-12971.
15. Barnes CP, Sell SA, Boland ED, Simpson DG, Bowlin GL. *Adv Drug Deliv Rev*., 2007 Dec 10; 59(14):1413-33.
16. Madhaiyan K, Sridhar R, Sundarrajan S, Venugopal JR, Ramakrishna S. *Int J Pharm*. 2013 Jan 28;444(1-2):70-76.

17. Wepener I, Richter W, van Papendorp D, Joubert AM. *J Mater Sci Mater Med.*, 2012 Dec;23(12):3029-40.

18. Ravichandran R, Seitz V, Reddy Venugopal J, Sridhar R, Sundarrajan S, Mukherjee S, Wintermantel E, Ramakrishna S. *Macromol Biosci.*, 2013 Jan 18. doi: 10.1002/mabi.201200391.

19. Qu F, Lin JM, Esterhai JL, Fisher MB, Mauck RL. *Acta Biomater.*, 2013 Jan 29. doi:pii: S1742-7061(13)00031-7.

20. Jayakumar R, Prabaharan M, Nair SV, Tamura H. Biotechnol Adv., 2010 Jan-Feb;28(1):142-50.

21. Benitez PL, Sweet JA, Fink H, Chennazhi KP, Nair SV, Enejder A, Heilshorn SC. *Adv Healthc Mater*., 2013 Jan;2(1):114-8. doi: 10.1002/adhm.201200115.

22. Chen L, Zhu C, Fan D, Liu B, Ma X, Duan Z, Zhou Y. *J Biomed Mater Res A*. 2011 Dec 1;99(3):395-409.

23. Su Y, Mo X. *J Contrl. Rel.,* 2011 Nov 30;152 Suppl 1:e230-2.

24. Bou-Akl T, Banglmaier R, Miller R, Vandevord P. *J Biomed Mater Res A*., 2013 Jan 28. doi: 10.1002/jbm.a.34549.

25. A. Marczak and Z. Jóźwiak. *Toxicol In Vitro.*, 2009, 23, 1188-1194.

26. J. C. Isenburg, D. T. Simionescu and N. R. Vyavahare. *Biomaterials,* 2005, **26**, 1237-1245.

27. http://www.moyak.com/papers/riboflavin-vitamin-B_2.html

28. http://www.healthbenefitsmadeez.com/b_2.html

29. G. Wollensak. *Curr Opin Ophthalmol*., 2006, **17**, 356-360.

30. E. Chan and G. R. Snibson. *Clin Exp Optom*., 2013, **7**, 1385–1396.

31. K. M. Meek and S. Hayes. *Ophthalmic Physiol Opt.,* 2013, **33**, 78-93.

32. M. Hovakimyan, R. F. Guthoff and O. Stachs. *J Ophthalmol.,* 2012, **2012**, 1-12, ID-406850.

33. M. O. Price, L. R. Tenkman, A. Schrier, K. M. Fairchild, S. L. Trokel and F. W. Price Jr. *J Refract Surg.,* 2012, **28**, 706-713.

34. Y. Goldich, A. L. Marcovich, Y. Barkana, Y. Mandel, A. Hirsh, Y. Morad, I. Avni and D. Zadok. *Cornea*, 2012, **31**, 609-614.

35. A. C. Renesto, L. A. Melo Jr, M. F. Sartori and M. Campos. *Am J Ophthalmol*., 2012, **153**, 982-993.

36. K. M. Bottos, A. G. Oliveira, P. A. Bersanetti, R. F. Nogueira, A. A. S. Lima-Filho, J. A. Cardillo, P. Schor, W. Chamon. *PLoS ONE*. 2013, **8**, e66408.

37. P. W. Morrison, C. J. Connon, V. V. Khutoryanskiy. *Mol Pharm*. 2013, **10**, 756-62.

38. Y.Z. Zhang, J. Venugopal, Z.-M. Huang, C.T. Lim, S. Ramakrishna. 2006, **47**, 2911–2917.

39. X. Li, M. A. Kanjwal, L. Lin and I. S. Chronakis. *Coll. and Surf. B: Biointerfaces*, 2013, **103**, 182 – 188.

40. M. Scott, K. Stefan, F. E. Henry, W. K. George, R. L. Richard, E. B. Helen, D. Zinaida, J. C. D. Megan, M. C. Ethan and W. C. Gary. *Invest Ophthalmol Vis Sci*., 2010, **51**, 129 –138.

FIGURE CAPTIONS

Figure. 1. Concept & hypothesis: Cross-linking of Gel microfiber mediated singlet oxygen from Riboflavin cross-linker.

Figure. 2. Morphology of Rib loaded nanofibers: a) SEM image of electrospun 1% Rib-Gel microfibers before CXLing. b) SEM image of electrospun 1% Rib-Gel microfibers after CXLing. c) SEM image of electrospun 5% Rib-Gel film before CXLing. d) SEM image of electrospun 5% Rib-Gel film after CXLing. e) SEM image of electrospun 1% Rib-PCL nanofiber. f) Magnified SEM image of electrospun 1% Rib-PCL nanofiber. g) AFM image of electrospun 5% Rib-Gel microfibers. g) 3D AFM image of electrospun 5% Rib-Gel microfibers.

Figure. 3. a) SEM image of freeze dried Fibrinogen hydrogel after treatment with 1% Rib-PCL nanofiber and UV CXLing. b) SEM image of freeze dried Gelatin hydrogel after treatment with 1% Rib-PCL nanofiber and UV CXLing. c) FT-IR spectrum of freeze dried Rib CXLed Fibrinogen hydrogel. d) FT-IR spectrum of Fibrinogen.

Figure. 4. Comparison of FT-IR spectra Rib loaded Gel and PCL nanofibers with the control polymer nanofibers. a) FT-IR spectrum of 5 % Rib-PCL nanofiber. b) FT-IR spectrum of PCL nanofiber. c) FT-IR spectrum of 5 % Rib-Gel microfiber after UV CXLing. d) FT-IR spectrum of 5 % Rib-Gel microfiber before UV CXLing. e) FT-IR spectrum of Gel microfiber.

Figure. 5. a) Contact angle measurements of 5% Rib-PCL nanofibers and the plasma treated samples. b) Cumulative vitamin B_2 release measurements using UV spectrophotometer show sustained release of vitamin B_2 from 5% Rib- PCL.

Figure. 6. Degradation studies of 5% Rib-PCL NFMs: a) Plasma and PBS untreated membranes. b) 60 minutes Plasma treated and PBS untreated membranes. c) Plasma

untreated and PBS soaked (for two months) Rib-PCL membranes. d) Plasma (60 min) and PBS (for two months) treated Rib-PCL membranes.

Figure. 7. Linear Tensile strength measurement of Rib-Gel microfibers. a) Tensile strength measurements show increase in vitamin loading or time of UV cross-linking increased the stability of Gel microfibers in comparison with Glutaraldehyde CXLed control. b) Increase in vitamin loading or time of UV cross-linking increased the young's modulus of Gel microfibers.

Figure. 8. Surface morphology of 5% Rib-Gel microfibers. a) AFM image showing surface of 5% Rib-Gel NFM before CXLing. b) AFM image showing surface of 5% Rib-Gel NFM after CXLing. c) Effect of crosslinking and mechanical strength as a measure of surface roughness of 5% Rib-Gel NFMs.

Figure. 9. UV light mediated singlet oxygen generation from Riboflavin and hydrogel formation as a result of Gel CXLing.

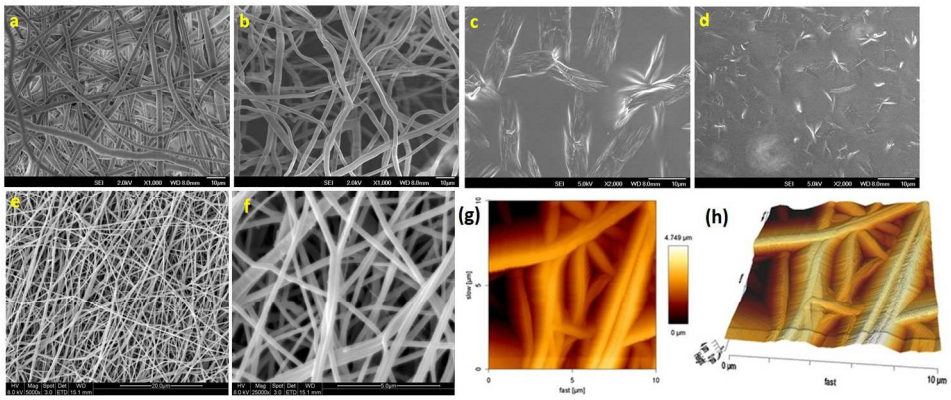

506x212mm (96 x 96 DPI)

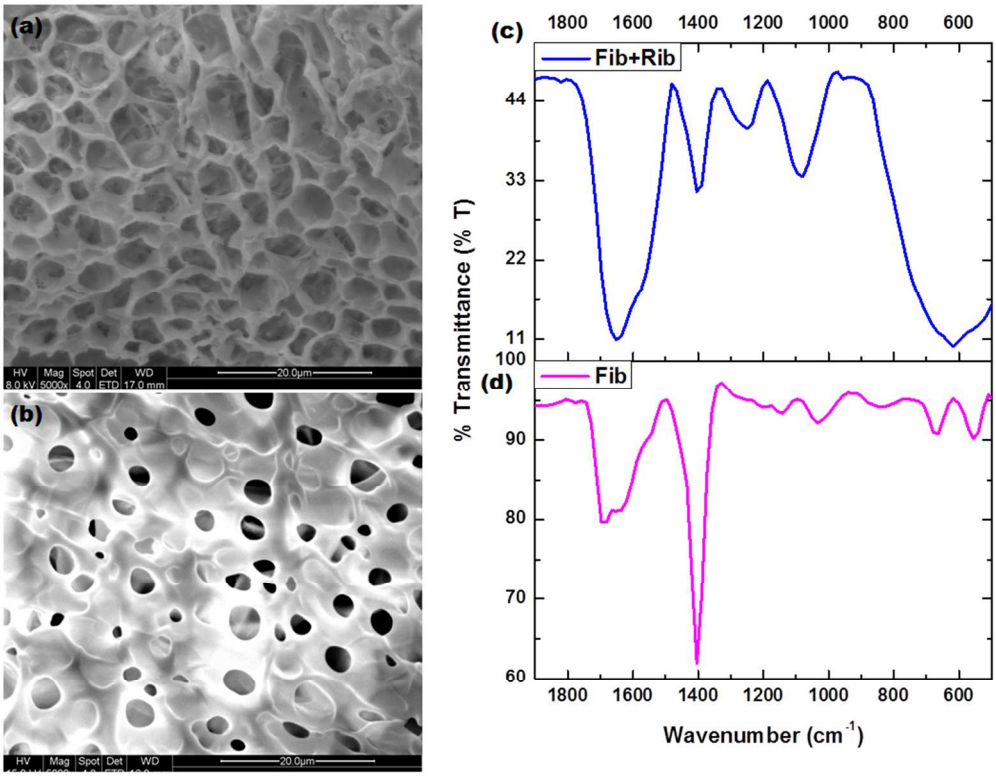

371x287mm (72 x 72 DPI)

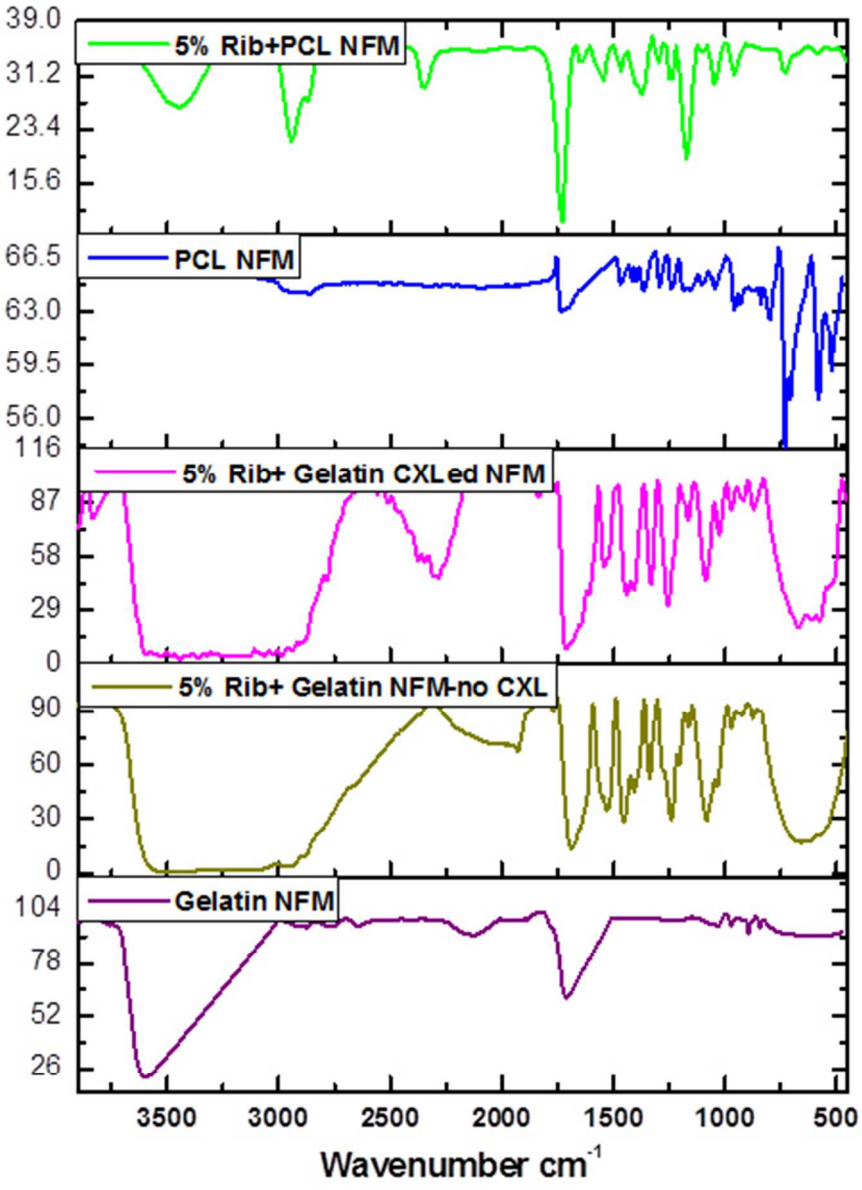

163x221mm (72 x 72 DPI)

Figure 5a

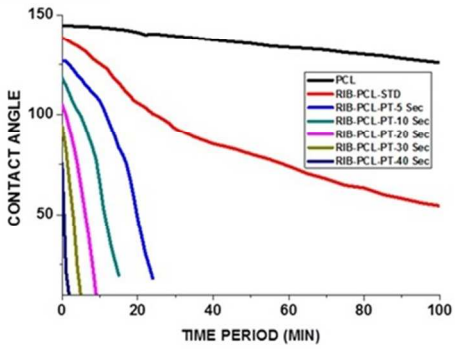

Figure 5b

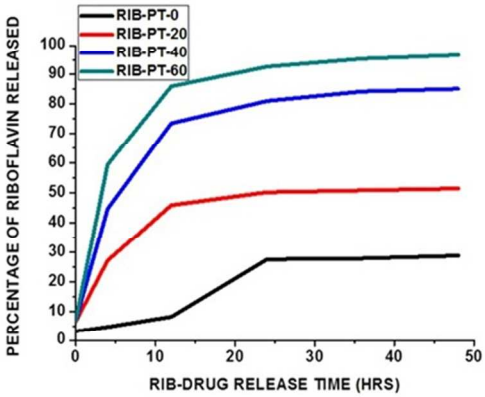

352x164mm (72 x 72 DPI)

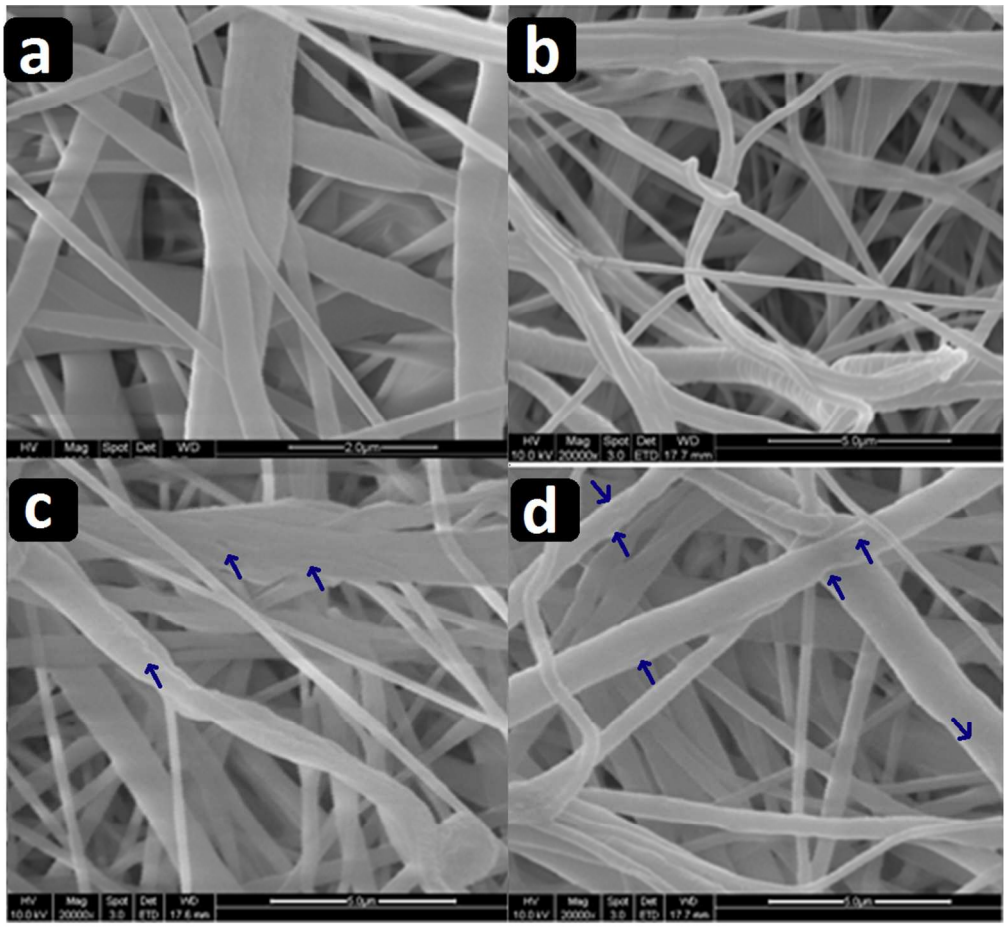

398x366mm (72 x 72 DPI)

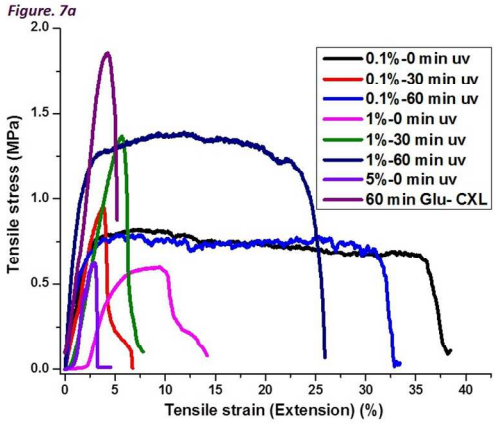

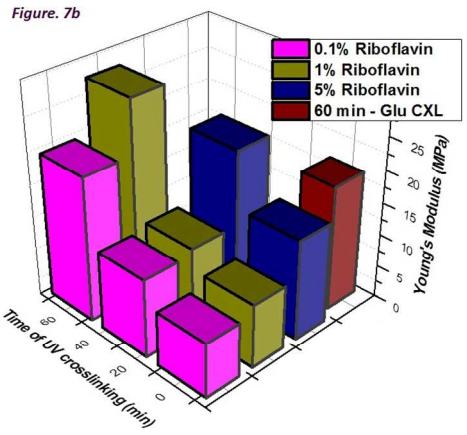

509x221mm (72 x 72 DPI)

Figure. 8a

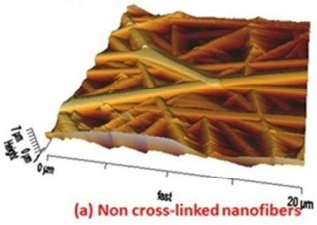

(a) Non cross-linked nanofibers

Figure. 8b

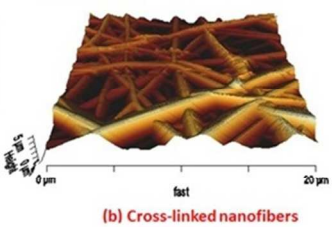

(b) Cross-linked nanofibers

Figure. 8c

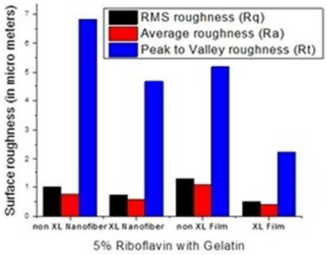

360x161mm (72 x 72 DPI)

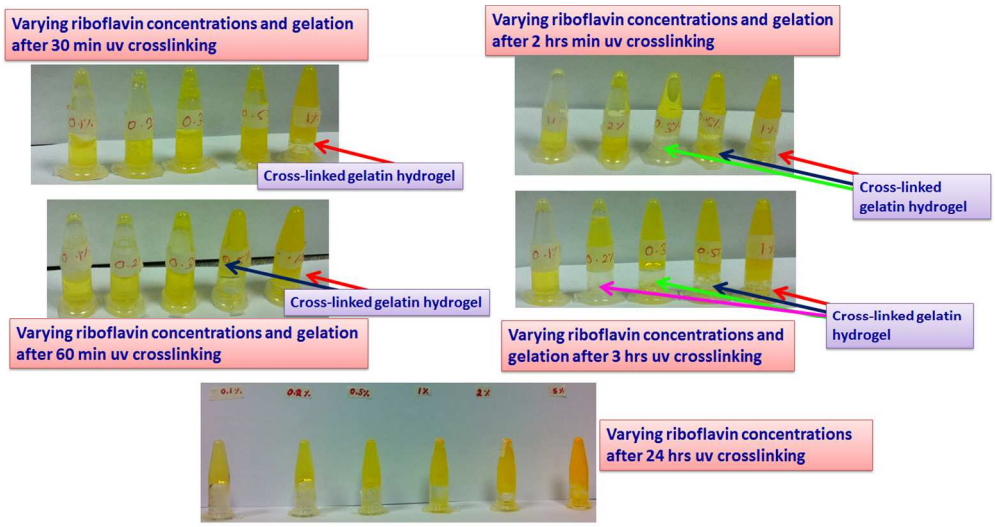

528x275mm (72 x 72 DPI)